J Biol Inorg Chem (2001) 6:120–127
DOI 10.1007/s007750000176

ORIGINAL ARTICLE

Catrin Hasselgren · Hyun Ik Park · Li-June Ming

Metal ion binding and activation of *Streptomyces griseus* dinuclear aminopeptidase: cadmium(II) binding as a model

Received: 13 December 1999 / Accepted: 15 September 2000 / Published online: 9 January 2001

Abstract A detailed metal binding and activation of the dinuclear aminopeptidase from *Streptomyces griseus* (sAP) has been analyzed and modeled by means of metal titration as well as kinetic and thermodynamic techniques using Cd^{2+} as a probe. Cd^{2+} binds to the two metal-binding sites in a sequential manner to produce a very active Cd^{2+}-substituted derivative, particularly in the presence of Ca^{2+} (53% and 90%, respectively, relative to the activities of the native form in terms of k_{cat}/K_m under the same conditions). The first stepwise formation constant for the binding of metal to the dinuclear site (to form M-sAP) was found to determine the metal-binding selectivity, regardless of the magnitude of the second stepwise formation constant (to form M,M-sAP from M-sAP). Interestingly, despite the seemingly very different binding profiles for different metal ions under different conditions, all of them can be well described and fitted by the sequential binding model. In addition, Ca^{2+} was found to significantly affect metal binding, inhibition, and entropy of activation of this enzyme, and its role in sAP action is re-evaluated.

Keywords Aminopeptidase · Dinuclear · Metal Binding · Streptomyces · Cadmium

C. Hasselgren · H.I. Park · L.-J. Ming (✉)
Department of Chemistry and Institute
for Biomolecular Science, University of South Florida,
Tampa, FL 33620-5250, USA
E-mail: ming@chuma.cas.usf.edu
Phone: +1-813-9742220
Fax: +1-813-9741733

Present address:
C. Hasselgren
Department of Inorganic Chemistry,
Chalmers University of Technology,
412 96 Gothenburg, Sweden

Introduction

The aminopeptidase from *Streptomyces griseus* (sAP) is a Ca^{2+}-regulated, thermo-stable, extra-cellular di-Zn^{2+} enzyme (MW=30 kDa), which prefers substrates with a large hydrophobic N-terminus [1, 2]. The ligand environments about the two Zn^{2+} ions (separated by 3.65 Å) in sAP are virtually identical, i.e., a five-coordinate environment consisting of one imidazole (His), one bidentate carboxylate (Asp or Glu), and one bridging Asp side chain, and possibly a hydroxide bridge (Fig. 1) [3]. Despite the great similarity in their coordination spheres, the two sites are distinguishable in terms of their metal binding as Co^{2+} can be introduced selectively to only one of the two sites at pH 6.1 [4]. This selectivity thus must derive from the amino acid side chains in the close proximity of the active site, such as Arg202 which is known to affect phosphate binding [5]. This selectivity in metal binding was also observed for the AP from *Aeromonas proteolytica* (aAP), whose activity was found to be strongly dependent on the order of metal addition [6, 7]. Since the metal-binding pattern of sAP depends on the

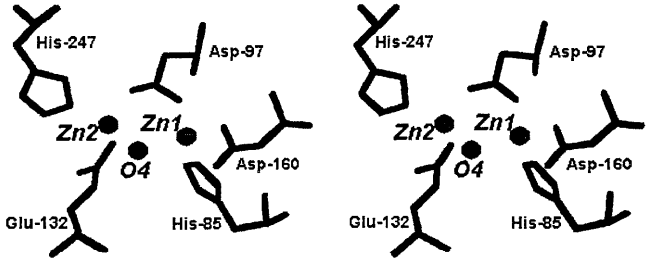

Fig. 1 The crystal structure of the active site of sAP (Protein Databank code 1xjo). The corresponding amino acids in aAP are Asp117 (bridging), Asp179 and His97 (Zn1), and Glu152 and His256 (Zn2). Only the bridging oxygen (O4) of the "bridging phosphate" suspected in the crystal structure is shown (however, see [5]), which is consistent with the bridging hydroxide in the aAP structure

metal ion (e.g., Co^{2+} versus Zn^{2+}) and is also significantly affected by the solution conditions (e.g., pH and $[Ca^{2+}]$) [4], it is thus important to investigate quantitatively the binding of metal ions to the dinuclear site in order to rationalize the apparently different metal-binding patterns.

The amino acid sequence of sAP has a low similarity to those of *Saccharomyces cerevisiae* AP and aAP (34.4% and 29.6%, respectively) [8]. However, the amino acids of the zinc binding sites in these three APs are conserved. Moreover, the overall folding of sAP resembles that of aAP, and the Zn^{2+} binding sites in these two APs are virtually identical (Fig. 1) [3, 9]. Some significant differences near the active site appear to be that Ile255 and Tyr225 in aAP are replaced by Tyr246 and Asp200, respectively, in sAP. Crystal structures also reveal that different side chains are involved in inhibitor (and probably substrate) binding, such as Tyr225 and Glu151 in aAP and Arg202, Glu131, and Tyr246 in sAP [3, 9, 10]. Consequently, the actions of these two APs are different because of these structural differences, despite their virtually identical metal binding coordination spheres. For example, aAP exhibits ~80% activity with only one metal ion bound, which is characteristic of mononuclear catalysis, and the second metal is involved in only substrate binding [6, 7, 11, 12], whereas sAP requires two metal ions for activity, characteristic of dinuclear catalysis [1, 2, 4].

The activities of several metal-substituted derivatives of sAP are significantly affected by Ca^{2+} [1, 2]. This regulation of activity by Ca^{2+} has not previously been observed for any other aminopeptidase. The Ca^{2+} site in sAP is located ca. 25 Å away from the active site according to the crystal structure [3]. This long distance makes it difficult to rationalize the relationship between the Ca^{2+} ion and the activity. Nevertheless, Ca^{2+} has been proposed to regulate the electrostatic potential distribution, but not to affect the conformation of the enzyme [3]. Recently, we found that Ca^{2+} also affected the selectivity of metal binding to the dinuclear site [4]. It is thus interesting to further address the effect of Ca^{2+} on the activity and metal-binding properties of sAP.

We report herein studies of metal-binding, kinetic, and thermodynamic properties of sAP and Ca^{2+} binding and the influence on these properties by the use of Cd^{2+} as a probe. The high activity of the Cd^{2+}-substituted derivative of sAP (90% and 53% with and without 2 mM Ca^{2+}, respectively) also justifies its use as a prototype for the study of sAP. Like Zn^{2+}, Cd^{2+} apparently shows much less selectivity than Co^{2+} toward the two metal-binding sites on the basis of the activity profiles during metal titrations. Nevertheless, we found that the Cd^{2+}-activity profile can be explained by a sequential binding mode. The significant influence of Ca^{2+} on metal binding, catalysis, and inhibition of sAP has also been investigated, and its role in sAP action is re-evaluated and discussed.

Materials and methods

Chemicals and materials

The substrate Leu-*p*-nitroanilide (Leu-*p*NA), the inhibitors bestatin and Leu-hydroxamate, EDTA, and all buffers were obtained from Sigma (St. Louis, Mo.). Cd^{2+} stock solutions were prepared from atomic absorption standard (99.99%, Fisher Scientific, Orlando, Fla.) or from metal salts of the highest purity (99.95%, Aldrich, Milwaukee, Wis.) standardized against standard EDTA using xylenol orange as an indicator. All solutions were prepared with de-ionized water of >18 MΩ from a Milli-Q system (Millipore, Bedford, Mass.). All glassware and plastic ware were treated with EDTA solution and rinsed with de-ionized water prior to use. The enzyme sAP was purified from Pronase (Fluka Chemika and Sigma) and its apo form was prepared according to the literature procedure [1, 2, 4].

Metal-binding studies

In Cd^{2+} activation of sAP, 0.5 mM Cd^{2+} solution was titrated into 5.0 μM apo sAP in 0.1 M MES at pH 6.0 or 0.1 M HEPES at pH 8.0 and the activities toward the hydrolysis of 1 mM substrate were monitored at 25 °C on a Varian Cary 3E spectrophotometer. The data were corrected for dilution and plotted as initial rate versus Cd^{2+} equivalent. The dependence of sAP activity on Ca^{2+} was studied under above conditions, in which Ca^{2+} solution was titrated into Cd,Cd-sAP and the initial rates for the hydrolysis of the substrate were measured and plotted against $\log[Ca^{2+}]$. The dependence of sAP activity on Cd^{2+} in the range from micromolar to millimolar was studied similarly.

Kinetic studies

All kinetic measurements were performed in 0.1 M HEPES at pH 8.0 with 60 mM $NaNO_3$ with or without 2 mM Ca^{2+} at 25 °C on the Cary 3E spectrophotometer. The activity of sAP was determined from the initial rate of Leu-*p*NA hydrolysis by monitoring the release of *p*NA (ε_{405}=10,500 M^{-1} cm^{-1}). The kinetic parameters k_{cat} and K_m were obtained by non-linear fitting of the initial rate V to the Michaelis-Menten equation $V=k_{cat}[S][E_0]/(K_m+[S])$, in which [S] is the substrate concentration and $[E_0]$ the initial enzyme concentration. For inhibition studies, the inhibitor Leu-hydroxamate was added to the assay cuvettes together with the substrate prior to the addition of sAP solution, and the activity was measured. The inhibition of bestatin was conducted with pre-incubation of the inhibitor with the enzyme overnight at 4 °C prior to the measurement of the activity.

In temperature-dependent kinetic studies, the sAP activity was determined every 10 °C between 20 and 70 °C in 0.1 M HEPES at pH 8.0 with 60 mM $NaNO_3$ in the presence or absence of 1 mM Ca^{2+}. The data were fitted directly to the Arrhenius equation below to obtain the activation energy E_a:

$$k_{cat} = A\exp(-E_a/RT) \quad (1)$$

where k_{cat} is obtained from the Michaelis-Menten equation, R is the gas constant, and T the temperature. Thermodynamic parameters for the reactions are obtained by the following relationships (Eqs. 2, 3, 4), with h the Planck constant and k_B the Boltzmann constant:

$$\Delta G^{\ddagger} = -RT\ln(k_{cat}h/k_B T) \quad (2)$$

$$\Delta H^{\ddagger} = E_a - RT \quad (3)$$

$$\Delta S^{\ddagger} = (\Delta H^{\ddagger} - \Delta G^{\ddagger})/T \quad (4)$$

Results and discussion

Cd^{2+} binding to sAP

Cd^{2+} is utilized as a probe in this study because its coordination chemistry closely resembles that of Zn^{2+}, which lacks ligand field stabilization energy and has a flexible coordination geometry due to its d^{10} electronic configuration. Despite their very different ionic radii (1.09 and 0.88 Å for six-coordinated Cd^{2+} and Zn^{2+}, respectively) [13], Cd^{2+} has been used successfully as a probe for the investigation of the structure and mechanism of several Zn^{2+} proteins [14]. The high activity of the Cd^{2+}-substituted derivative of sAP (90% and 53% with and without 2 mM Ca^{2+} at pH 8.0, respectively) justifies its use as a probe for the study of sAP. However, it is interesting to note that Cd^{2+} does not restore to a great extent the activity of most enzymes that have been studied [15]. The activity of the di-Zn^{2+} aminopeptidase from bovine lens is also not restored by Cd^{2+} [16], whereas that of aAP is regenerate only to 22% by Cd^{2+} [6]. Although several transition metal ions may also serve as useful probes for the study of the spectroscopically silent Zn site in proteins, distortion of the active site geometry has been observed in some cases resulting from ligand field stabilization energy contribution and different geometric preferences, such as in Ni^{2+}-substituted derivatives of carboxypeptidase A and astacin [17, 18]. The binding of Co^{2+} to sAP is selective and sequential at pH 6.1, based on the results from optical, NMR, and activity studies [4]. It would be interesting if this binding pattern could be generalized for the interpretation of the binding of Cd^{2+} and other metal ions to sAP.

The binding of Cd^{2+} to sAP under various conditions is monitored via activity toward the hydrolysis of Leu-*p*NA. The binding of only two equivalents of Cd^{2+} to sAP is clearly shown at pH 8.0, in which the activity reaches maximum at >2 equivalents of Cd^{2+} (Fig. 2A). At pH 8.0 in the absence of Ca^{2+} the enzyme exhibits 33% activity upon binding of one equivalent of Cd^{2+} relative to that with 2 equivalents of Cd^{2+} (○, Fig. 2A), suggesting the formation of the corresponding mole fraction of the active Cd,Cd-sAP. At pH 6.0 in the absence of Ca^{2+} (○, Fig. 2B) the binding of Cd^{2+} to sAP is also sigmoidal, which exhibits 20% relative activity with 1 equivalent Cd^{2+} bound (reflecting that the formation of Cd,Cd-sAP is less preferred at lower pH). The binding profiles are still sigmoidal in the presence of Ca^{2+} at both pH 8.0 and 6.0, showing 40% and 30% relative activity, respectively, upon binding of 1 equivalent Cd^{2+} (●, Fig. 2). An ideal selective metal binding to one of the two binding sites should exhibit no activity with less than 1 equivalent of metal ion if the di-metal derivative is the only active form of the enzyme, whereas a completely cooperative binding should afford ~50% activity with 1 equivalent of metal bound relative to that with 2 equivalents of metal. These Cd^{2+} binding-activity profiles are quite different from the nearly selective Co^{2+} binding pattern reported previously [4]. Whether or not all of these activity profiles of different metal ions under different conditions can be described by a generalized metal-binding mechanism is not obvious at this stage, which are further analyzed in the next section.

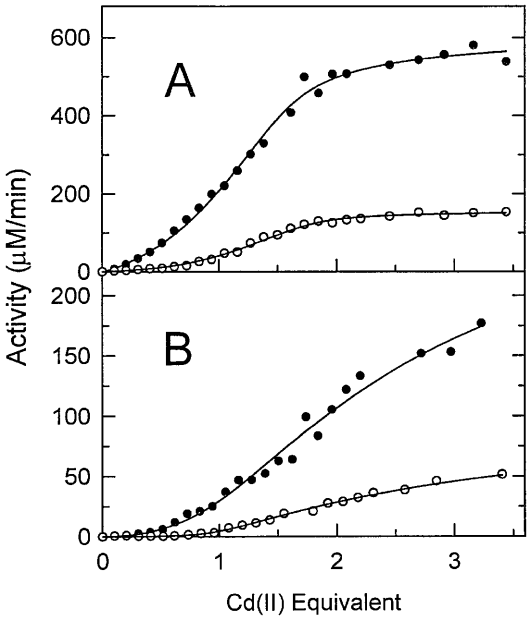

Fig. 2 Activity of 0.5 μM apo sAP upon titration of Cd^{2+} at **A** pH 8.0 and **B** pH 6.0 in the presence (●) and absence (○) of 2 mM Ca^{2+}. The *solid traces* are the best fits of the data to the sequential metal binding model shown in Eq. 5

Metal-binding modes of sAP

The sigmoidal activity profiles for Cd^{2+} binding suggest the presence of a partial selectivity, as it is approaching the ideal selective metal-binding mode described above[1]. Since the two metal-binding sites have very similar geometry and ligand type (Fig. 1), the selectivity must be attributed by some neighboring groups discussed in the Introduction. We attempt to describe the several different metal-binding patterns by the use of a straightforward two-step sequential binding mode with a few assumptions based on Co^{2+} binding that have been verified with activity and spectroscopies [4]:

[1] In other words, the sigmoidal binding patterns seem perfect to be described by a cooperative binding mode. However, the classical cooperative binding describes the binding of ligands to identical binding sites as in the case of multi-subunit proteins like hemoglobin. Since the two metal-binding sites in sAP are in fact different (despite their very similar ligand types), the term "selectivity" is chosen to avoid confusion with the classical definition of two identical sites in cooperative binding

1. The metal ion selectively binds to only one site, but not to both the two sites in a parallel fashion.
2. The binding is sequential.
3. Once the first metal ion is bound, the binding of metal ion to the empty second site proceeds.
4. The only active form is the di-metal form.

This sequential binding mode can be described by the two equilibria shown in Eq. 5:

$$\mathrm{sAP} \overset{\mathrm{M(II)}}{\underset{K_1}{\rightleftharpoons}} \mathrm{M-sAP} \overset{\mathrm{M(II)}}{\underset{K_2}{\rightleftharpoons}} \mathrm{M,M-sAP} \qquad (5)$$

in which M(II) is assumed to bind selectively to one site of the dinuclear center (the first equilibrium) followed by the binding to the second site (the second equilibrium) with two stepwise apparent formation constants, K_1=[M-sAP]/[sAP][M] and K_2=[M,M-sAP]/[M-sAP][M]. The amount of M,M-sAP formed can be easily monitored with the activity. Selective and sequential metal binding to a dinuclear center under different conditions (e.g., pH and anions) has also been previously observed in other proteins, including the analogous aminopeptidase aAP [6, 7] and Cu,Zn-superoxide dismutase [19, 20, 21]. Expression of the activity in terms of [M,M-sAP] can be achieved by substitution of [M-sAP] as a function of the initial metal concentration. Despite the very different shapes of the profiles acquired at two different pH values in the presence and absence of Ca^{2+} (● and ○ , respectively, Fig. 2), they can all be satisfactorily fitted to this sequential metal-binding mode (solid traces).

Although Co^{2+} binding to sAP has been proved to be selective and to produce an inactive Co_1-sAP and active Co,Co-sAP by means of optical and NMR spectroscopies and activity assay [4], it cannot be concluded whether or not Cd^{2+} binds exclusively to one site over the other to form an active or inactive mono-Cd-substituted derivative (i.e., Cd,E-sAP or E′,Cd-sAP with E the empty site, or a mixture of both derivatives). In this case, the two formation constants should be treated as apparent formation constants. An alternative fitting of the Cd-binding profiles is also attempted in which the mono-Cd-substituted derivatives are assumed active, i.e., rate=f_1[Cd_1-sAP]+f_2[Cd,Cd-sAP]. Nearly identical K_1, K_2, and f_2 values are obtained with very small or negligible f_1 values, i.e., f_1/f_2=4.8% and ~0% at pH 8.0 with and without Ca^{2+}, and 0.85% and 0.02% at pH 6.0 with and without Ca^{2+}, respectively. Significantly larger standard deviations (>2-fold) are also obtained in these fittings. The results suggest that the assumption that the mono-Cd derivatives are inactive is valid to a great extent, and is followed here for the discussion of Cd^{2+} binding.

In the sequential binding model, the activity of the enzyme should depend on both the magnitude and the relative value of the stepwise formation constants K_1 and K_2. A large value of K_1 should result in a selective binding mode since only one metal-binding site is preferentially filled to afford the "non-catalytic" M-sAP; and a large K_2 value should cause a deep rise in activity upon metal binding (particularly at greater than 1 equivalent) since the active M,M-sAP can be formed effectively. This metal-binding model is numerically simulated to afford a better visualization of the correlation between the activity profile and the two stepwise formation constants, and for better comparison of the data from the current and previous studies (Fig. 3).

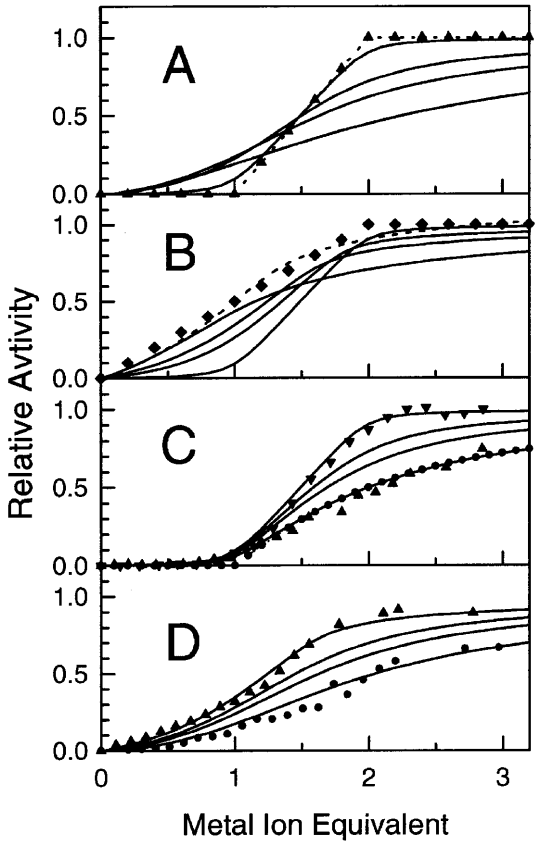

Fig. 3A–D Simulations of metal binding to sAP according to the equilibria in Eq. 5 with the two stepwise formation constants K_1 and K_2. An arbitrary full activity of 1.0 "activity unit" from an enzyme sample of 1.0 "concentration unit" is chosen in all the simulations, which affords relative magnitude of the values. The values of K_1/K_2 (*solid traces* from top to bottom at 2 equivalents) are 100/100, 10/10, 5/5, and 2/2 in **A**, 100/100, 10/100, 5/100, and 2/100 in **B**, 100/100, 100/10, 100/5, and 100/2 in **C**, and 5/100, 5/10, 5/5, and 5/2 in **D**. The *solid circle trace* in **C** represents a completely selective metal binding to the first site and a much weaker metal binding to the second site (i.e., $K_1/K_2=10^6/2$), which can be fitted well to the sequential binding model (*dotted trace*). Two extreme cases are shown, a sequential binding with a full selectivity (i.e., no activity at <2 equivalents, ▲ in **A**) and a simultaneous binding of 2 metal ions with no selectivity (i.e., with an extremely strong positive cooperativity, ◆ in **B**). The *dotted traces* are the best fits of these two cases according to the sequential binding. The former can be perfectly fitted whereas the latter cannot, reflecting the validity of the model for the description of sequential metal binding. Normalized metal-binding profiles for Co^{2+} (▼ in **C** [4]) and Cd^{2+} (▲ in **C**, from Fig. 2) at pH 6.0 in the presence of Ca^{2+}, Cd^{2+} at pH 8.0 with Ca^{2+} (● in **D**, from Fig. 2), and Zn^{2+} at pH 8.5 with Ca^{2+} (▲ in **D** [4]) are also shown for comparison

A constant K_1/K_2 ratio

In this case, both K_1 and K_2 are varied simultaneously. It shows that the selectivity decreases when both constants decrease (from top to bottom at 2 equivalents). Under an extreme case where the binding of the two metal ions is completely selective (i.e., activity is 0 at [M] less than 1 equivalent; ▲ in Fig. 3A), it can be still perfectly fitted by the sequential binding pattern (dotted trace), which demonstrates the validity of the model.

$K_1 \leq K_2$ (constant)

In this case, K_2 is kept constant while K_1 value is varied to reveal the effect of K_1 on metal binding. It is clearly shown that a smaller K_1 results in a significant activity when 1 equivalent of metal ion is introduced. This is because a smaller K_1 value would leave more free metal ions available for the empty site to form M_2-sAP. It seems likely that the extreme case where 2 metal ions bind to the dinuclear site simultaneously (i.e., with an extremely strong positive cooperativity; ◆ in Fig. 3B) might be fitted with a small K_1 and a large K_2. However, the fitting of the data to the model in Eq. 5 is not satisfactory (dotted trace).

K_1 (constant) $\geq K_2$

When K_1 is relatively large, selective metal binding to form the inactive M_1-sAP becomes evident regardless of the magnitude of K_2 (Fig. 3C). This is because only a small amount of free metal ion is available for the second site when less than 1 equivalent metal ion is added. Consequently, when the K_1 value is extremely large, the second site would be completely empty (and no activity would be detected) until more than 1 equivalent of metal ion is added, as shown by the solid circles in Fig. 3C. This hypothetical extreme case can be perfectly fitted with the sequential binding model (dotted trace), indicating the validity of the model. In this case, the activity is solely dependent on the formation constant K_2. The selective binding of Co^{2+} to sAP observed previously [4] can also be described quite well by the binding profiles shown in Fig. 3C (▲, normalized Co^{2+} binding profile at pH 6.1 without Ca^{2+} [4], not fitted). The most selective Cd^{2+} binding mode (pH 6.0 without Ca^{2+}) is also in this category (▲, normalized data from Fig. 2B, ○), as shown by its values of $K_1 > K_2$ (Table 1).

Small K_1 values

The variation of K_2 with respect to a small K_1 is shown in Fig. 3D, in which the loss of selectivity to form the inactive M_1-sAP is obvious. The Zn^{2+} binding pattern observed previously [4] can also be described with this binding situation (▲, normalized Zn^{2+} binding profile at pH 8.5 in the presence of Ca^{2+} [4], not fitted). The activity profiles for Cd^{2+} binding at pH 8.0 in the presence of Ca^{2+} are similar to that of Zn^{2+} (however, with a smaller relative K_2 value, as shown by the normalized binding profile ●), suggesting that Cd^{2+} can be a good substitute for the study of Zn^{2+} binding and activation of sAP. Interestingly, the binding pattern of the native metal ion Zn^{2+} reflects that Zn^{2+} can actually be very effective in activating sAP, since the activity can be acquired with less than 1 equivalent Zn^{2+}, particularly in the presence of Ca^{2+} (cf. trace ▲). The Ca^{2+} influence is further discussed in a later section.

The Cd^{2+} binding profiles of sAP under different conditions are seemingly quite distinct, as reflected by their activity profiles. However, all can be fitted well by the sequential binding model (solid traces, Fig. 2). The stepwise formation constants for Cd^{2+} binding to apo sAP obtained from the fittings of the activity profiles are listed in Table 1. At pH 8.0, K_2 values are about the same with and without Ca^{2+}, whereas K_1 decreases by 50% in the presence of Ca^{2+}, which accounts for the decrease in metal-binding selectivity. Both K_1 and K_2 change significantly when the pH is lowered to 6.0 in the absence of Ca^{2+}, i.e., K_1 increases by four times, which enhances the selectivity of Cd^{2+} binding (cf. Fig. 3B), while K_2 decreases by nearly 100 times, which accounts for the weak Cd^{2+} binding to Cd-sAP (thus requiring more than 2 equivalents of Cd^{2+} to exhibit full activity)[2]. In the presence of Ca^{2+} at pH 6.0, K_1 drops to the level of that at pH 8.0, which accounts for the significant loss in metal-binding selectivity, whereas K_2 does not change significantly. Cd^{2+} binding is much more influenced by pH than by Ca^{2+}. At pH 8.0, deprotonation of a coordinated water may occur, which can reduce charge repulsion between the two metal ions in the dinuclear site. In the meantime, the deprotonated water (hy-

Table 1 Stepwise formation constants for 0.2 μM Cd^{2+} binding to 5.0 μM sAP obtained according to Eq. 5

	K_1 (μM^{-1})	K_2 (μM^{-1})	f (min^{-1})[a]
pH 8.0 (–Ca^{2+})	19.9±1.8	101.4±19.9	319
pH 8.0 (+Ca^{2+})	10.0±0.8	106.5±4.6	1230
pH 6.0 (–Ca^{2+})	81.2±27.7	1.1±0.2	197
pH 6.0 (+Ca^{2+})	17.2±8.2	1.5±0.6	647

[a] Conversion factor which reflects the relative initial rate resulting from each titration when the two metal-binding sites are fully occupied by Cd^{2+} under the experimental conditions

[2] A ^{113}Cd-reconstituted sAP at pH 6.0 did not exhibit characteristic ^{113}Cd NMR signals, reflecting the weak binding characteristics of Cd^{2+} and the presence of a fast chemical exchange between the free and bound Cd^{2+}. This negative result also precludes the characterization of the one-Cd derivative as Cd,E-sAP or E′,Cd-sAP, or a mixture of both

droxide) may be attracted to the Cd^{2+} in the second site and form a bridging ligand, thus increasing the second stepwise formation constant K_2.

Ca^{2+} binding and effect

It is interesting to reveal that Ca^{2+} not only affects the metal-binding pattern (●, Fig. 2), but also significantly enhances the activity of Cd,Cd-sAP (by affecting k_{cat} and K_m, see below), as in the case of the native enzyme observed previously [1, 2, 22]. The combination of these influences makes Ca^{2+} an ideal regulator for sAP, since the enzyme can acquire the same level of activities at lower metal ion concentrations in the presence of Ca^{2+} than is the case without Ca^{2+} under the same conditions. The influence of Ca^{2+} on sAP activation is clearly shown in the activity profiles at pH 6.0 and 8.0 (Fig. 2 and Table 1), which can be also visualized in Ca^{2+} titration profiles. At pH 8.0, the maximum activity is reached at $[Ca^{2+}]\approx 1$ mM (●, Fig. 4). A fitting of the activity profile according to the following equilibrium (Eq. 6) for a single Ca^{2+} binding gives a formation constant K_f=20.4 mM^{-1}:

$$\mathrm{Ca(II)} + \mathrm{M,M-sAP} \rightleftharpoons \mathrm{Ca(II)-M,M-sAP} \qquad (6)$$

At pH 6.0, however, the activity approaches maximum at higher $[Ca^{2+}]$: ca. 10 mM with K_f=1.2 mM^{-1} at $[Cd^{2+}]$=0.1 mM (▲), and 3.2 mM^{-1} at $[Cd^{2+}]$=2 μM (■). The lower apparent affinity constants at pH 6.0 can be attributed to H^+ binding to the Ca^{2+} binding site, and the decrease in the magnitude at higher Cd^{2+} concentration (0.1 mM, ▲) suggests that Cd^{2+} may compete for the Ca^{2+} binding site. Since Cd^{2+} has been demonstrated to be a good substitute for Ca^{2+} in several proteins [23], the exchangeability of these two metal ions is further studied and discussed below.

The enzyme reaches nearly full activity with the introduction of 2 equivalents of Cd^{2+} in the presence of Ca^{2+} at pH 8.0 (Fig. 2A). In the absence of Ca^{2+}, however, an excess amount of Cd^{2+} is needed to reach the magnitude of activity approaching that in the presence of Ca^{2+} (○, Fig. 4). A fitting of the data to the above equilibrium with Ca^{2+} replaced by Cd^{2+} affords an affinity constant K_f=44.1 mM^{-1} for the binding of the "excess Cd^{2+}" to Cd,Cd-sAP. Similar activation by the excess Cd^{2+} is also revealed at pH 6.0 (□, Fig. 4), yet with a smaller K_f of 8.3 mM^{-1}. This effective activation upon Cd^{2+} binding to the Ca^{2+} site with a large affinity constant suggests that Cd^{2+} can serve as a good substitute for Ca^{2+} in sAP.

The kinetic parameters of Cd,Cd-sAP toward Leu-*p*NA hydrolysis at pH 8.0 are dramatically affected by Ca^{2+}, i.e., the second-order rate constant (in terms of k_{cat}/K_m) is greatly enhanced owing to a 2-fold increase in k_{cat} and 7-fold decrease in K_m (Fig. 5 and Table 2). The influence of Ca^{2+} on the activity of native and Co,Co-sAP was reported previously [1, 2, 4]. However, the mechanism for this influence could not be concluded, and was suspected to be due to an electrostatic effect of the Ca^{2+} ~25 Å away from the active site based on the crystal structure study [3]. In order to gain further insight into the dramatic effects of Ca^{2+} on metal binding and activation of sAP, the inhibition and temperature-dependent kinetics of the enzyme in the presence and absence of Ca^{2+} were further analyzed and are discussed below.

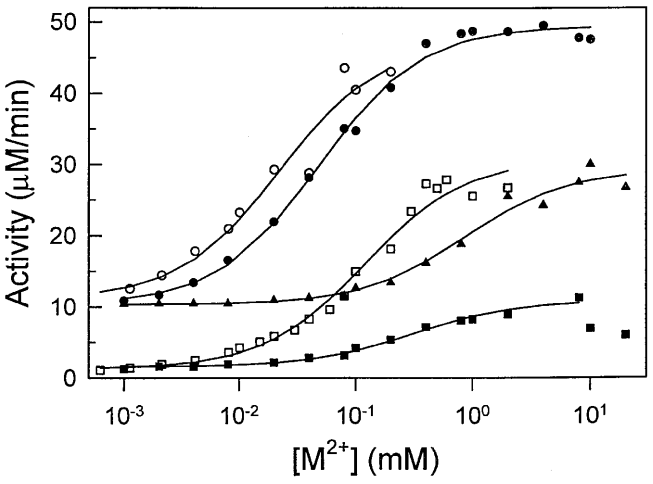

Fig. 4 The Ca^{2+}-dependent activity of 0.05 μM Cd,Cd-sAP at pH 8.0 and $[Cd^{2+}]$=0.125 μM (●), at pH 6.0 and $[Cd^{2+}]$=0.1 mM (▲), and at pH 6.0 and $[Cd^{2+}]$=2 μM (■); and the Cd^{2+}-dependent activity of 0.05 μM Cd,Cd-sAP at pH 8.0 (○) and pH 6.0 (□) in the absence of Ca^{2+}. The *solid traces* are the best fits of the data to the equilibrium of Eq. 6, giving formation constants of 20.4, 1.2, 3.2, 44.1, and 8.3 mM^{-1}, respectively. Higher Ca^{2+} concentrations cause a decrease in the activity; thus the data are not used in the fitting

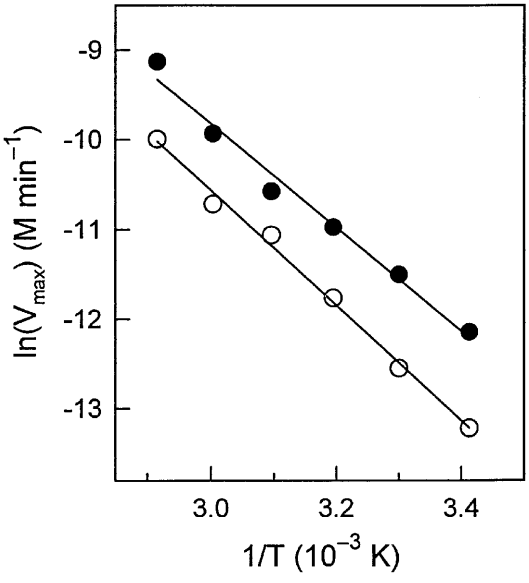

Fig. 5 Linear Arrhenius plots of Leu-*p*NA hydrolysis by sAP in the presence (●) and absence (○) of 1 mM Ca^{2+}. The activation energy values are obtained by non-linear fittings of the data to the Arrhenius equation (Eq. 1)

Table 2 Michaelis-Menten kinetic parameters and some thermodynamic parameters of activation (at 25 °C) for the hydrolysis of Leu-*p*NA by Cd,Cd- and Zn,Zn-sAP in the presence and absence of 2 mM Ca^{2+} at pH 8.0

	k_{cat} (s^{-1})	K_m (mM)	k_{cat}/K_m ($M^{-1}\,s^{-1}$)	E_a (kJ mol^{-1})	$\Delta H^{\ddagger}$ (kJ mol^{-1})	$\Delta S^{\ddagger}$ (J $mol^{-1}\,K^{-1}$)	$\Delta G^{\ddagger}$ (kJ mol^{-1})
Cd,Cd-sAP	15.6	0.35	0.045×10^6	53.3	50.9	–56.3	67.6
Cd,Cd-sAP+Ca^{2+}	35.6	0.050	0.71×10^6	53.1	50.6	–48.3	65.0
Zn,Zn-sAP [1, 2]	254	3.0	0.085×10^6	–	–	–	–
Zn,Zn-sAP+Ca^{2+}	433[a]	0.55[a]	0.79×10^{6a}	41.3[b]	38.8[b]	–53.3[b]	57.4[b]
Zn,Zn-aAP[c]	78.7	0.023	3.4×10^6	36.5	34.0	–94.2	62.1

[a] In the presence of 1 mM Ca^{2+} [1, 2, 22], and was found to be further enhanced in the presence of 2 mM Ca^{2+} [27]

[b] Obtained from [27]

[c] See [6, 7, 11, 12]

Inhibition studies

Inhibition of Cd,Cd-sAP by L-Leu-hydroxamate is competitive both in the presence and absence of Ca^{2+}, exhibiting inhibitor constants K_i of 1.6±0.1 and 4.6± 1.0 μM, respectively. Ca^{2+} clearly exerts a similar influence on the binding of inhibitor and substrate, i.e., a significant decrease in both the inhibitor constant K_i and the Michaelis constant K_m. This similarity suggests that this inhibitor may be recognized by the enzyme in a similar fashion as the substrate.

The bidentate hydroxamates of amino acids and peptides have been widely used as inhibitors for metalloproteases through binding to the active site metal(s) [24]. The crystal structure of a hydroxamate-bound aAP has recently been solved, which showed that the hydroxyl group acted as a bridging ligand while the carbonyl group interacted with only one Zn^{2+} [10]. The D-amino group of the hydroxamate was shown to form a H-bond with Tyr225 in aAP. The corresponding position in sAP is occupied by Asp200 [1, 2, 3, 9], which would be too short and have a wrong stereochemistry for such H-bonding. It seems unlikely that L-Leu-hydroxamate may bind to sAP in a similar fashion as the binding of the D-form inhibitor to aAP. Nevertheless, a direct binding of the inhibitor to the metal ion(s) can be expected, as observed in other cases [24]. The exact binding mode of hydroxamate with sAP remains to be seen in future structural studies.

The inhibition of Cd,Cd-sAP by bestatin ([(2*S*,3*R*)-3-amino-2-hydroxy-4-phenylbutanoyl]-L-leucine) is also competitive with and without Ca^{2+}. This can be expected as bestatin is a transition state analogue with a tetrahedral β-hydroxyl moiety which is bound to the active-site metal ions in a bidentate fashion through the 2-hydroxyl and the 3-amino groups, as revealed in the crystal structure of bestatin-bound bovine lens aminopeptidase [25, 26]. This binding mode resembles the transition-state α-amino-*gem*-diolate structure. The K_i values were found to be 7.1±5.3 and 73±12 nM in the presence and absence of Ca^{2+}, respectively. This large Ca^{2+} influence on K_i corresponds well to the significant Ca^{2+} influence on K_m, which suggests that bestatin binding to sAP may mimic substrate binding.

The mechanism for the dramatic Ca^{2+} effect on sAP catalysis is to stabilize the transition state complex via specific interactions (to increase k_{cat}), and to enhance effective substrate binding to the enzyme (to decrease K_m). Interaction of Ca^{2+} with the *gem*-diolate moiety seems to be a reasonable mechanism to stabilize the transition state. However, as the *gem*-diolate-like configuration is not present in both inhibitors, Ca^{2+} interaction with the *gem*-diolate may not be the case. Further investigations are needed to reveal the detailed interactions associated with the Ca^{2+} effect on sAP catalysis.

Temperature dependence of kinetics

The temperature-dependent study of the hydrolysis reveals that the difference in the catalytic rates in the presence and absence of Ca^{2+} is caused by the entropy of activation $\Delta S^{\ddagger}$, as the enthalpy of activation $\Delta H^{\ddagger}$ is not changed (Table 2). The entropy change is –48.3 J K^{-1} mol^{-1} in the presence of Ca^{2+}, and –56.3 J K^{-1} mol^{-1} without Ca^{2+}. The less negative $\Delta S^{\ddagger}$ in the presence of Ca^{2+} can be attributed to a tighter substrate binding (with a smaller K_m value, Table 2), which results in a loss of molecular motion in the ground state enzyme-substrate complex. This would afford a smaller difference in entropy between the ground and transition states, thus a less negative $\Delta S^{\ddagger}$, which results in a smaller free energy of activation $\Delta G^{\ddagger}$.

The thermodynamic parameters for the hydrolysis of Leu-*p*NA by native Zn,Zn-sAP [27] in the presence of Ca^{2+} and by aAP [11, 12] are also reported for comparison (Table 2). Although the entropy contributions of –53.3 and –94.2 J K^{-1} mol^{-1} in Zn,Zn-sAP and aAP catalysis are less favorable than in Cd,Cd-sAP catalysis under the same conditions, they are compensated by much lower values of $\Delta H^{\ddagger}$ to afford favorably low Gibbs free energies of activation [11, 12, 27].

The thermal stability of sAP seems not to be affected by Ca^{2+} under the conditions in this study (<65 °C). Thus, Ca^{2+} may not play a significant structural role, but acts more as a regulator in sAP action. The crystal structures of sAP in the presence and absence of Ca^{2+} are virtually identical and the Ca^{2+} binding site is intact in the absence of Ca^{2+}, also reflecting that Ca^{2+} may not be involved in structural

stabilization. Moreover, the relatively weak Ca^{2+} binding to Cd,Cd-sAP and to native sAP [1, 2] also support the regulatory role of Ca^{2+}.

Conclusion

The metal binding and activation properties of the dinuclear sAP have been revealed in this study using Cd^{2+} as a probe, which can also explain Co^{2+} and Zn^{2+} binding and activation patterns. The study indicates that the metal binding is consecutive and its selectivity is determined by the first stepwise formation constant K_1, and is not influenced by K_2. The influences of Ca^{2+} and pH on metal binding and activation of sAP have been established quantitatively according to this binding mode. Moreover, the Ca^{2+} effect on catalysis was found to be attributed to the decrease in the magnitude of $\Delta S^{\ddagger}$. These significant Ca^{2+} effects on sAP properties do not seem to be satisfactorily explained by the previously suspected electrostatic effect caused by the Ca^{2+} ca. 25 Å away from the active site [1, 2, 22]. Further investigation on the unique Ca^{2+} effect is needed.

We have recently observed that sAP exhibits an unexpected "alternative activity" toward the hydrolysis of the phosphodiester bis(*p*-nitrophenyl) phosphate, with an enormous ~10^{10} times enhancement of the first-order rate constant [28]. Since Cd^{2+} and Zn^{2+} have different ligand preferences due to their different softness, Cd,Cd-sAP may serve as a potential candidate for future investigation of this unique catalysis on "alternative substrates" to provide further insight into the mechanistically distinct dinuclear hydrolyses of peptides and phosphoesters in chemical and biological systems.

Acknowledgements This study is partially supported by the Petroleum Research Funds administrated by the American Chemical Society (ACS-PRF no. 35313-AC3). The support by the University of South Florida (USF) on this study is also acknowledged. C.H. gratefully acknowledges funding from the National Board of Student Aid in Sweden (CSN) during a visit to USF as partial fulfillment of the requirements for a BS degree from Uppsala University.

References

1. Spungin A, Blumberg S (1989) Eur J Biochem 183:471–477
2. Ben-Meir D, Spungin A, Ashkenazi R, Blumberg S (1993) Eur J Biochem 212:107–112
3. Greenblatt HM, Almog O, Maras B, Spungin-Bialik A, Barra D, Blumberg S, Shoham G (1997) J Mol Biol 265:620–636
4. Lin L-Y, Park HI, Ming L-J (1997) JBIC 2:744–749
5. Harris MN, Ming L-J (1999) FEBS Lett 455:321–324
6. Prescott JM, Wagner FW, Holmquist B, Vallee BL (1985) Biochemistry 24:5350–5356
7. Bayliss ME, Prescott JM (1986) Biochemistry 25:8113–8117
8. Maras B, Greenblatt HM, Shoham G, Spungin-Bialik A, Blumberg S, Barra D (1996) Eur J Biochem 236:843–846
9. Chevrier B, Schalk C, D'Orchymont H, Rondeau J-M, Moras D, Tarnus C (1994) Structure 2:283–291
10. Chevrier B, D'Orchymont H, Schalk C, Tarnus C, Moras D (1996) Eur J Biochem 237:393–398
11. Chen G, Edwards T, D'souza VM, Holz RC (1997) Biochemistry 36:4278–4286
12. Bennet B, Holz RC (1997) J Am Chem Soc 119:1923–1933
13. Cotton FA, Wilkinson G (1988) Advanced inorganic chemistry, 5th edn. Wiley, New York
14. Summers MF (1988) Coord Chem Rev 86:43–134
15. Bertini I, Luchinat C (1994) In: Bertini I, Gray HB, Lippard SJ, Valentine JS (eds) Bioinorganic chemistry, University Science Books, Sausalito, Calif., pp 37–106
16. Allen MP, Yamada AH, Carpenter FH (1983) Biochemistry 22:3778–3783
17. Rees DC, Howard JB, Chakrabarti P, Yeates T, Hsu BT, Hardman KD, Lipscomb WN (1986) In: Bertini I, Luchinat C, Maret W, Zeppezauer M (eds) Zinc enzymes, chap 10. Birkhauser, Boston
18. Gomis-Rüth F-X, Grams F, Yiallouros I, Nar H, Küsthardt U, Zwilling R, Bode W, Stöcker W (1994) J Biol Chem 269:17111–17117
19. Ming L-J, Valentine JS (1987) J Am Chem Soc 109:4426–4428
20. Ming L-J, Valentine JS (1990) J Am Chem Soc 112:4256–4264
21. Ming L-J, Valentine JS (1990) J Am Chem Soc 112:6374–6383
22. Papir G, Spungin-Bialik A, Ben-Meir D, Fudim E, Gilboa R, Greenblatt HM, Shoham G, Lessel U, Schomburg D, Ashkenazi R, Blumberg S (1998) Eur J Biochem 258:313–319
23. Vogel HJ, Forsén S (1987) Biol Magn Reson 7:249–309
24. Wilkes SH, Prescott JM (1983) J Biol Chem 256:13517–13521
25. Kim HD, Burley SK, Lipscomb WN (1993) J Mol Biol 230:722–724
26. Burley SK, David PR, Sweet RM, Taylor A, Lipscomb WN (1992) J Mol Biol 224:113–140
27. Park HI (1999) PhD dissertation, University of South Florida
28. Park HI, Ming L-J (1999) Angew Chem Int Ed Engl 38:2914–2916; Angew Chem 111:3097–3100